Publications

Available Online

J. Sci. Res. **15** (1), 121-129 (2023)

JOURNAL OF SCIENTIFIC RESEARCH

www.banglajol.info/index.php/JSR

Engineering of Aberrated PSF by Asymmetric Apodization with the Complex Shaded Aperture

M. Venkanna[1*], N. Sabitha[2], D. K. Sagar[2]

[1]Department of Physics, BVRIT Hyderabad College of Engineering for Women, Hyderabad, India

[2]Optics Research Group, Department of Physics, Osmania University, Hyderabad, India

Received 20 June 2022, accepted in final revised form 7 August 2022

Abstract

The point spread function (PSF) produced by a coherent optical system under the influence of defocus, coma, and primary spherical aberration (PSA) is examined in this work. This paper deals with asymmetric apodization and pupil engineering to control monochromatic aberrations. To reduce the influence of monochromatic aberrations on the diffracted PSF, this approach uses amplitude and phase apodization. Analytical investigations on intensity PSF are carried out with varying amounts of aberrations and degrees of amplitude and phase apodization. Computed central peak intensity and full width at half maxima (FWHM) and analyzed. The resolution of a diffraction-limited optical imaging system is improved by using an asymmetric optical filter that minimizes the effect of defocus.

Keywords: Aberrations; Asymmetric apodization; Optical filters; Resolution.

doi: http://dx.doi.org/10.3329/jsr.v15i1.60366 J. Sci. Res. **15** (1), 121-129 (2023)

1. Introduction

Apodization is the process of suppressing optical side-lobes in the diffraction field of an optical imaging system [1-4]. For enhancing the depth of focus, phase apodization is used [5-7]. The efficiency of the apodization technique is always associated with the design of the pupil function. As reported in the earlier works [8-13], asymmetric apodization is the simultaneous suppression of optical side-lobes and sharpening of the main peak of the PSF. In this case, however, the lobes on the good side of the PSF were completely suppressed at the expense of extended side lobes; on the bad side, the resultant PSF that is asymmetric is crucial in confocal imaging [14]. The focal point of a high-aperture focusing system can also be reduced by employing vortex phase functions [15,16]. A substantial number of studies have been conducted on asymmetric apodization [17-21]. In confocal scanning systems or optical imaging systems, asymmetric apodization is used to achieve axial and lateral resolution. It is technically possible to detect the image of extrasolar planets directly. It is evident that asymmetric apodization alters the distribution of light flux enclosed in the diffraction pattern and provides the resolution of an optical

* *Corresponding author*: venkioptics@gmail.com

system [22]. PSF engineering is the manipulation of light distribution in the focal region of an optical system and is used to improve the performance of optical systems for many applications [23-25]. This approach modifies the size of the focal spot and the level of its neighboring side-lobes, as demonstrated by inserting an appropriate phase filter, amplitude filter, or both in the Fourier plane of the given optical system [26-29]. Optical aberrations reduce the overall performance of an optical system [30,31]. Aberrations can be reduced by using an optical element with a high optical transmission function [32-42]. Traditionally, apodization of the exit pupil of the optical system has been aimed at producing a high-quality output or increasing imaging qualities. PSFs from aberrated lenses is greatly distorted, providing a serious concern in a wide range of optical applications. Therefore, the generation of a smooth intensity PSF profile has become one of the keynotes of contemporary imaging systems underneath aberrations. In this context, the coherent optical system with the recommended apodization technique aims to reduce aberration effects and enhance the resolving power. The resulting center peak of the PSF, corresponding to the given point object, is being detected longitudinally shifted due to defocus rather than at the diffraction focus, resulting in a decrease in central peak intensity [43]. A spherical aberration of the lens, on the other hand, influences the resultant intensity PSF of the point image due to a difference in optical ray paths from the source to the focus, i.e., the peripheral rays of the lens do not converge into exact focus relative to the paraxial rays [44]. It is evident that spherical aberration reduces the intensity of the central peak, increases the intensity of the first-order side lobe, and shifts the first minima location between the central peak and the first-order side lobe. Therefore, defocusing and spherical aberrations play a critical role in defining the PSF of an optical system because they have severely distorted PSF. An aberration-free lens pupil forms the Airy PSF, with most incident light energy concentrated in the central region, or Airy disc, and the rest scattered among the side lobes.

In this paper, a one-dimensional shaded aperture is designed and divided into three zones: Applied phase apodization for the two narrow edge strips and, in the central zone, applied amplitude apodization to modify the spatial distribution of light intensity in the image plane of the optical system. By employing asymmetric apodization, the impulse response of an optical system under defocus, coma, and primary spherical aberrations is obtained. The optical system chosen in this paper is considered to be linear, shift variant diffraction limited, and asymmetric. The relation between the coded image and PSF is accomplished mathematically. The current study has a wide range of applications in astronomical observations, confocal imaging, medical imaging, optical communications, adaptive optics, etc.

2. Design and Mathematical Formulation

In optical systems, a diffracted image is a spatial pattern of light dispersion in the image plane. The last aspect of the image resolution evaluation is whether or not the image permits the detector to recognize the axial shape of the point spread function in the

presence of wave aberrations in the pupil plane of the optical system with the appropriate amplitude and phase apodizer. The Fourier Transform of the pupil functions is used in the situation of one-dimensional amplitude and phase apodizer impulse responses of optical systems. The schematic representation of an asymmetric optical imaging system with a circular aperture is shown in Fig. 1.

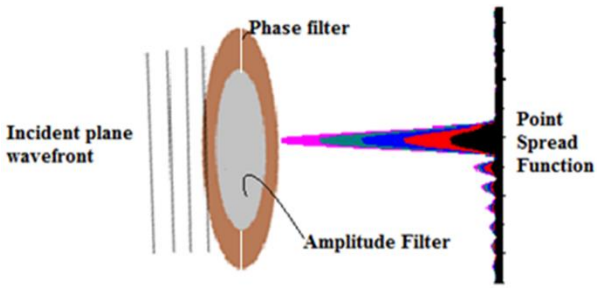

Fig. 1. General schematic representation of optical imaging system.

The optical system consists of a circular aperture of two circular strips of equal width; one is opaque, and the other is transparent. Due to the deep suppression ability and constant operational angles throughout the edge zones, they impose phase functions that are complex conjugate. The central zone of the aperture is opaque. In the presence of monochromatic aberrations such as coma, primary spherical aberration, and defocus, the total diffraction amplitude transmittance A (Z) into the image plane is equal to the sum of the individual phase transmittances contributed by the edge strips for which amplitude transmittance is unity and the amplitude transmittance contributing by the central zone of the pupil functions of width (1 – 2S) apodized by shaded aperture is given by

$$\left.\begin{aligned} &Left\ Opaque = e^{-i\pi/2}, \quad -0.5 \le r < -0.5 + S, \\ &Central\ mask = 1 - \beta r^2, \quad -0.5 + S \le r \le 0.5 - S, \\ &Right\ Opaque = e^{+i\pi/2}, \quad 0.5 - S < r \le 0.5 \end{aligned}\right\} \tag{1}$$

On introducing the wave aberrations such as defocus, coma, and primary spherical aberrations, the complex amplitude impulse response of the optical system with one-dimensional amplitude and phase filter is given as

$$A(Z) = \int_{-0.5}^{-0.5+S} -i\exp(i2Zr)dr + \int_{-0.5+S}^{0.5-S} (1-\beta r^2)\exp(-i(\phi_d \frac{r^2}{2} + \phi_c \frac{r^3}{3}\cos\theta + \phi_s \frac{r^4}{4})dr + \int_{0.5-S}^{0.5} i\exp(i2Zr)dr \tag{2}$$

The intensity PSF formed by an apodized optical system is given by the squared modulus of expression (2)

$$B(Z) = |A(Z)|^2 \tag{3}$$

The resultant amplitude distribution of light A (Z) in the focal region of the one-dimensional optical imaging system is equal to the sum of diffraction amplitudes of three zones. Here Z = (2π/λ) sin θ, r is the coordinate in the aperture function; 'Z' is the quantity that has a dimension of inverse wavelength units; λ is the wavelength of the monochromatic light incident. φ_d, φ_c and φ_s are the defocus, coma, and primary spherical aberration quotients, respectively. The width of the edge strip (S) is a parameter determined from the minimum of the square of the intensity in the side-lobe range. In this case, the side-lobe region is stated by 'Z', which is connected to the angle of orientation θ. S is the control parameter of phase apodization or asymmetric apodization, or width of the edge strips.

The pupil function of the shaded aperture is given by $\boldsymbol{f(r) = 1 - \beta r^2}$

The level of non-uniformity of the transmission over the exit pupil is controlled by the degree of amplitude apodization β. It accepts a range of numbers from 0 to 1. For β = 0, it is obvious that f(r) =1, implying uniform transmittance over the exit pupil. The amplitude transmittance of this apodizer falls monotonically from the center to the margins of the pupil. This phenomenon is depicted in further detail in Fig. 2. Due to apodization, the pupil transmittance at the margins is lower than at the center, resulting in a reduction of higher spatial frequency components in the image. This is manifested as partial or complete reduction of undesirable optical side lobes or secondary maxima, which improves imaging characteristics. It is evident from this that the shaded aperture is the best apodizer for circular apertures.

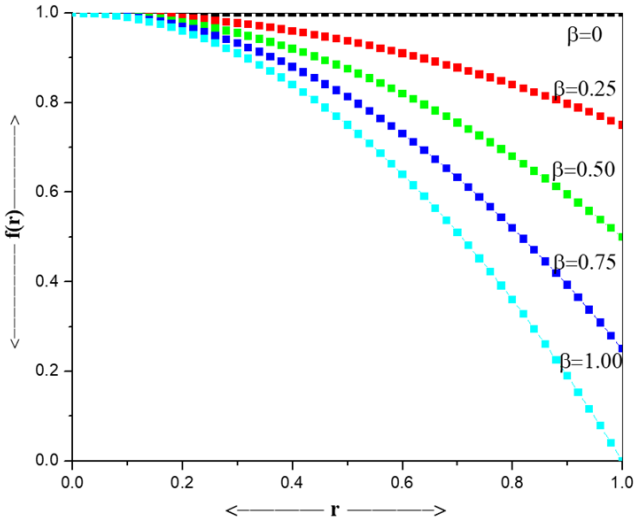

Fig. 2. Amplitude transmittance of the shaded aperture with various values of β.

3. Results and Discussion

The effects of asymmetric apodization on the PSF formed by coherent optical systems apodized by the amplitude filter and phase filter in the presence of defocus, coma, and primary spherical aberrations for several values of the dimensionless diffraction variable Z ranging from -10 to 10, the intensity distribution B (Z) in the image of point objects have been obtained. Only one side of the diffracted image, known as the PSF's good side (right side), is computed. On the other side, the PSF has narrowed the central peak and repressed the side lobes. In the presence of monochromatic aberrations, the lateral resolution of the PSF in terms of the central peak width or its FWHM is evaluated for various degrees of amplitude and phase apodization.

The influence of Coma and PSA on the performance of the shaded aperture on coherent optical systems in the formation of PSF images has been investigated. The degree of coma φ_c and PSA φ_s considered are π and 2π. By considering unapodized (β=0) and apodized (β ≠ 0) pupil functions, the intensity distribution of aberrated PSF has been computed at the planes of (defocus) φ_d=0, π, and 2π. These figures demonstrate the intensity profile of the PSF in the presence of aberrations.

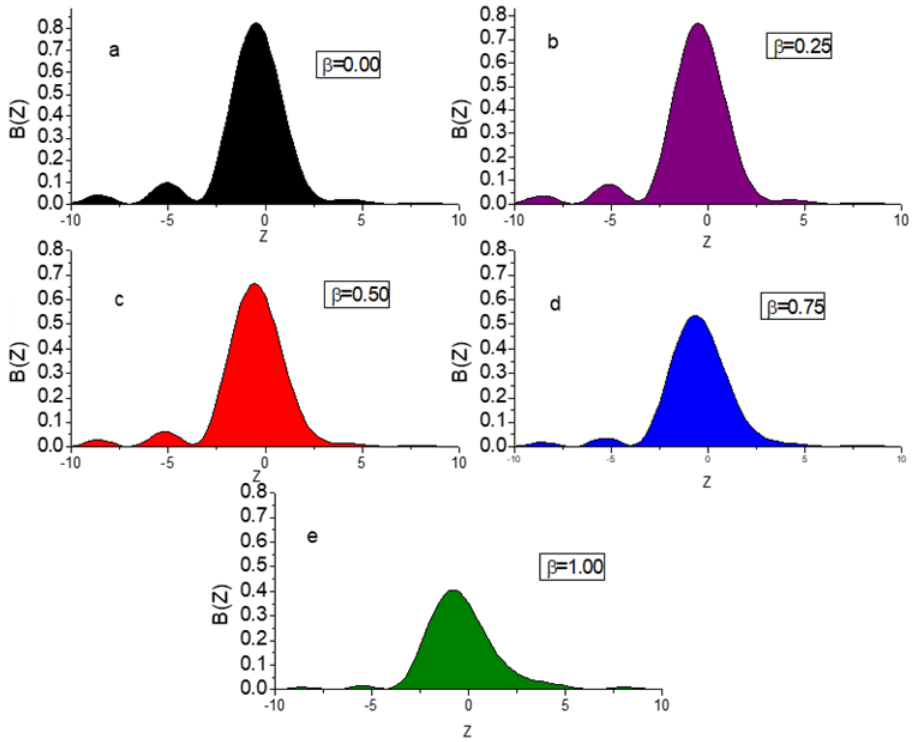

Fig. 3. Intensity PSF profiles in the presence of defocus (φ_d=2π), coma (φ_c=2π), and PSA (φ_s=2π), under asymmetric apodization(S=0.05) for different levels of apodization (a) β=0, (b) β=0.25, (c) β=0.5, (d) β=0.75 and (e) β=1.

Fig. 3 shows the shape of the aberrated PSF for various amplitude apodization values while the phase apodization is held constant. In the presence of amplitude apodization, the side lobes on the good side are greatly decreased and completely erased, even for β = 0 (Fig. 3a) (from Figs. 3b-3e). The pupil function becomes more successful in translating the spatial intensity distribution into the PSF with improved axial resolution when apodization β = 0.5, as seen in Fig. 3c. Even when there are a lot of monochromatic aberrations, the utilized asymmetric apodization across the pupil removes the side lobes on the good side, resulting in a smooth intensity PSF.

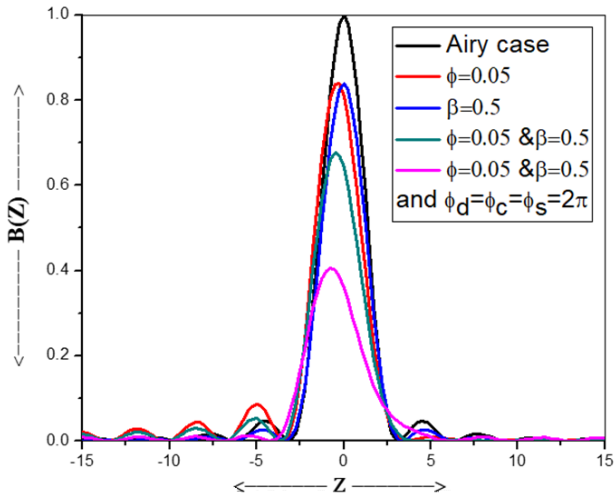

Fig. 4. Intensity PSF under asymmetric apodization for aberration-free and aberrated systems.

Fig. 4 illustrated the light intensity distribution under various considerations and compared with the Airy case (solid black line). It is observed that for aberration-free PSF subjected to both the amplitude (β=0.5) and phase(S=0.05) apodization, optical side lobes are almost removed, and the central peak is narrowed on the good side of the pattern, whereas in the presence of a high degree of defocus, coma and PSA, the central peak is broadened.

Fig. 5(A) illustrates the normalized intensity distributions of PSF along the propagation direction at the planes of φ_d=0, π, and 2π (from left to right) underneath aberrations of coma φ_c=π and PSA φ_s= π. It is observed that the normalized intensities at the planes φ_d=0, π, and 2π are 0.6662, 0.6601 and 0.6436, respectively. The FWHM is a useful metric for describing the size of a focal point spot. The FWHM at the planes φ_d=0, π, and 2π are 3.15, 3.15, and 3.17, respectively. Fig. 5(B) shows the corresponding intensity PSF when a coma φ_c=2π and PSA φ_s= 2π. From Fig. 5(B), it is observed that the normalized intensities at the planes φ_d=0, π, and 2π are 0.6571, 0.6501, and 0.6327, respectively, and the FWHM at the planes φ_d=0, π, and 2π are the same and are 3.2 (from Table 1). It is a significant achievement that at these chosen planes, the optical system

shows almost similar imaging characteristics and is hence useful in long focal depth applications.

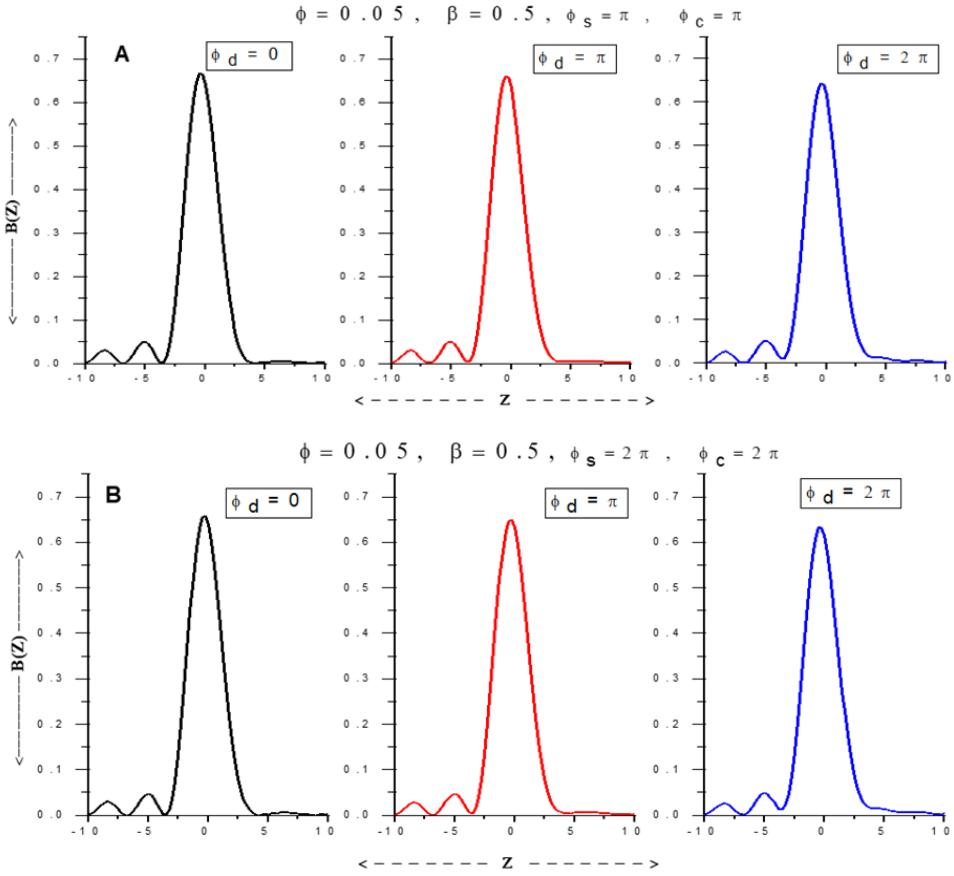

Fig. 5. Intensity PSF at different planes φ_d =0, π, and 2π for β=0.5 and S=0.05 (A) when coma φ_d=π and PSA φ_s= π, (B) when coma φ_c=2π and PSA φ_s= 2π.

Table 1. Central peak intensity and FWHM values of asymmetrically Apodized PSF.

Central peak intensity			FWHM	
φ_d	β=0.5 S=0.05 φ_s=φ_c= π	β=0.5 S=0.05 φ_s=φ_c=2π	β=0.5 S=0.05 φ_s=φ_c= π	β=0.5 S=0.05 φ_s=φ_c=2π
0	0.6662	0.6572	3.15	3.2
π	0.6601	0.6501	3.15	3.2
2π	0.6436	0.6327	3.17	3.2

4. Conclusion

The characteristics of an aberrated optical system under asymmetric apodization have been demonstrated theoretically. The resolution of PSF has been studied by employing

amplitude and phase apodization at focused and defocused planes in the presence of a high degree of coma and PSA. It is observed that for amplitude apodization β=0.5 and phase apodization S=0.05 the optical side lobes vanish on the good side even in the presence of aberrations. As a result, this effect implies giving super-resolution to two closely spaced objects with different brightness. It is emphasized that for the given considerations, the effect of defocus becomes insignificant, and the PSF has almost the same normalized peak intensity and FWHM. The design of such a complex shaded aperture is possible by deposition of the metallic and dielectric coating on a glass substrate and for metasurfaces. It is very useful for high contrast astronomical imaging, spectroscopy, and extended depth of focus imaging applications.

References

1. J. P. Mills and B. J. Thompson edited, Selected Papers on Apodization: Coherent Optical Systems (Bellingham, Washington: SPIE Optical Engineering Press, 1996).
2. P. Jacquinot and B. Roizen-Dossier, Prog. Optics **3**, 29 (1964). https://doi.org/10.1016/S0079-6638(08)70570-5
3. R. Barakat, J. Opt. Soc. Am. **52**, 276 (1962). https://doi.org/10.1364/JOSA.52.000276
4. R. Barakat, J. Opt. Soc. Am. **52**, 264 (1962). https://doi.org/10.1364/JOSA.52.000264
5. E. R. Dowski and W. T. Cathey, Appl. Opt. **34**, 1859 (1995). https://doi.org/10.1364/AO.34.001859
6. C. Pan, J. Chen, R. Zhang, and S. Zhuang, Opt. Exp. **16**, ID 13364 (2008). https://doi.org/10.1364/OE.16.013364
7. S. N. Khonina and A. V. Ustinov, Pattern Recognit. Image Anal. **25**, 626 (2015). https://doi.org/10.1134/S1054661815040100
8. L. Cheng and G. G. Siu GG, Measur. Sci. Tech. **2**, 198 (1991). https://doi.org/10.1088/0957-0233/2/3/002
9. G. G. Siu, L. Cheng, and D. S. Chiu, J. Phys. D: Appl. Phys. **27**, 459 (1994). https://doi.org/10.1088/0022-3727/27/3/005
10. A. N. K. Reddy and D. K. Sagar, Pramana **84**, 117 (2015). https://doi.org/10.1007/s12043-014-0828-0
11. G. G. Siu, M. Cheng, and L. Cheng, J. Phys. D: Appl. Phys. **30**, 787 (1997). https://doi.org/10.1007/s003400050230
12. M. N. Zervas and D. Tarvener, Fiber Integrated Opt. **19**, 355 (2000). https://doi.org/10.1080/014680300300001707
13. A. N. K. Reddy and D. K. Sagar DK, Adv. Opt. Tech. **1608342** (2016).
14. W. Yang and A. B. Kotinski, The Astrophys. J. **605**, 892 (2004). https://doi.org/10.1086/382586
15. S. N. Khonina, N. L. Kazanskiy, and S. G. Volotovsky, J. Mod. Opt. **58**, 748 (2011). https://doi.org/10.1080/09500340.2011.568710
16. S. N. Khonina, N. L. Kazanskiy, and S. G. Volotovsky, Opt. Memory Neural Networks **20**, 23 (2011). https://doi.org/10.3103/S1060992X11010024
17. M. K. Goud, R. Komala, A. N. K. Reddy, and S. L. Goud, Acta Physica Polonica A **122**, 90 (2012). https://doi.org/10.12693/APhysPolA.122.90
18. A. N. K. Reddy and D. K. Sagar, J. Info. Commun. Converg. Eng. **12**, 83 (2014). https://doi.org/10.6109/jicce.2014.12.2.083
19. A. N. K. Reddy and D. K. Sagar, Optica Pura y Aplicada **46**, 215 (2013). https://doi.org/10.7149/OPA.46.3.215
20. M. Kowalczyk, C. J. Zapata-Rodriguez, and M. Martinez-Corral, Appl. Opt. **37**, 8206 (1998). https://doi.org/10.1364/AO.37.008206

21. W. Yang and A. B. Kotinski, Astrophys. J. **605**, 892 (2004). https://doi.org/10.1086/382586
22. A. N. K. Reddy, D. K. Sagar, and S. N. Khonina, Comput. Opt. **41**, 484 (2017). https://doi.org/10.18287/2412-6179-2017-41-4-484-488
23. M. Venkanna and K. D. Sagar, Proc. SPIE **9654**, A1, (2015).
24. M. Venkanna and K. D. Sagar, Comput. Opt. **46**, 388 (2022). https://doi.org/10.18287/2412-6179-CO-940
25. A. N. K. Reddy and V. Pal, Appl. Phys. B **125**, 231 (2019). https://doi.org/10.1007/s00340-019-7345-2
26. A. N. K. R. Eddy and D. K. Sagar, Pramana–J. Phys. **84**, 117 (2015). https://doi.org/10.1007/s12043-014-0828-0
27. A. N. K. Reddy and D. K. Sagar, Adv. Opt. Tech. **2016**, ID 1608342 (2016).
28. M. Kowalczyk, C. J. Zapata-Rodriguez, and M. Martinez-Corral, Appl. Opt. **37**, 8206 (1998). https://doi.org/10.1364/AO.37.008206
29. S. C. Biswas and A. Boivin, Opt. Acta **23**, 569 (1976). https://doi.org/10.1016/0014-4835(76)90164-0
30. L. Magiera and M. Pluta, Opt. Appl. **11**, 231 (1981).
31. I. Escobar, G. Saavedra, M. Martinez-Corral, and J. Lancis, J. Opt. Soc. Am. A **23**, 3150 (2006). https://doi.org/10.1364/JOSAA.23.003150
32. M. Ruphy and O. M. Ramahi, J. Opt. Soc. Am. A **33**, 1531 (2016). https://doi.org/10.1364/JOSAA.33.001531
33. J. P. Mills and B. J. Thompson, J. Opt. Soc. Am. A **3**, 694 (1986). https://doi.org/10.1364/JOSAA.3.000694
34. L. N. Hazra, P. Purkait, and M. De, Can. J. Phys. **57**, 1340 (1979). https://doi.org/10.1139/p79-183
35. L. Pueyo, N. J. Kasdin, and S. Shaklan, J. Opt. Soc. Am. A **28**, 189 (2011). https://doi.org/10.1364/JOSAA.28.000189
36. C. Ratnam,V. L. Rao, and S. L. Goud, J. Phys. D **39**, 4148 (2006). https://doi.org/10.1088/0022-3727/39/19/005
37. D. K. Sagar, G. Bikshamaiah, and S. L. Goud, J. Mod. Opt. **53**, 2011 (2006). https://doi.org/10.1080/09500340600787507
38. M. Martinez-Corral, M. T. Caballero, E. H. K. Stelzer, and J. Swoger, Opt. Exp. **10**, 98 (2002). https://doi.org/10.1364/OE.10.000098
39. N. Reza and L. N Hazra, J. Opt. Soc. Am. A **30**, 189 (2012). https://doi.org/10.1364/JOSAA.30.000189
40. J. Campos, F. Calvo, and M. J. Yzuel, J. Opt. **19**, 135 (1988). https://doi.org/10.1088/0150-536X/19/3/005
41. A. N. K. Reddy and D. K. Sagar, Int. J. Opt. **2016**, ID 1347071 (2016).
42. L. N. Hazra and N. Reza, Pramana –J. Phys. **75**, 855 (2010). https://doi.org/10.1007/s12043-010-0167-8
43. A. N. K. Reddy, M. Hashemi, and S. N. Khonina, Pramana **90**, ID 77 (2018). https://doi.org/10.1007/s12043-018-1566-5
44. J. W. Goodman, Introduction to Fourier Optics, 3rd Edition (McGraw-Hill, New York, 2005).